Accurate Study of the Two Lowest Singlet States of HN3: Stationary Structures and Energetics at the MRCI Complete Basis Set Limit

ARTICLE *in* THE JOURNAL OF PHYSICAL CHEMISTRY A · APRIL 2013

Impact Factor: 2.69 · DOI: 10.1021/jp402090s · Source: PubMed

2 AUTHORS:

Breno Galvão
Centro Federal de Educação Tecnológica de M…
16 PUBLICATIONS **73** CITATIONS
SEE PROFILE

Antonio J. C. Varandas
University of Coimbra
382 PUBLICATIONS **6,749** CITATIONS
SEE PROFILE

THE JOURNAL OF PHYSICAL CHEMISTRY A

Article

pubs.acs.org/JPCA

Accurate Study of the Two Lowest Singlet States of HN_3: Stationary Structures and Energetics at the MRCI Complete Basis Set Limit

B. R. L. Galvão and A. J. C. Varandas*

Departamento de Química, Universidade de Coimbra, 3004-535 Coimbra, Portugal

ABSTRACT: The two lowest singlet potential energy surfaces of the hydrazoic acid are explored using high-level quantum chemistry calculations, revealing isomeric forms, transition states, and a new path for the nitrogen ring-closing mechanism in the ground state. The reaction of cyc-N_3 with hydrogen is shown to proceed through a barrierless path that dissociates to N_2 + NH($^1\Delta$) without reaching the HN_3 global minimum. Several intersections between the two states are localized for both N_3 isomers near the N_3 + H dissociation. The energies of stationary structures and dissociation asymptotes are obtained with the multireference configuration interaction method at the complete basis set limit. A comparison with recent experimental data regarding the H−N_3 bond strength and the dissociation barrier in the excited state shows that the present results are of chemical accuracy (~1 kcal mol^{-1}).

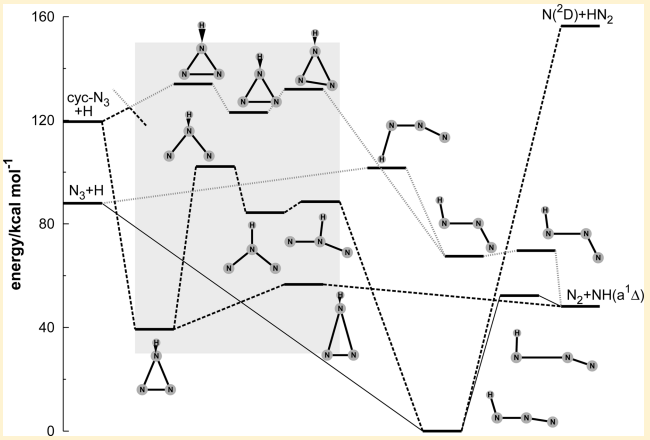

1. INTRODUCTION

The hydrazoic acid (HN_3) is a species of growing concern in the atmosphere due to its pollutant character[1] and belongs to a class of energetic molecules. Its decomposition in the lowest electronic state

$$HN_3(\tilde{X}^1A') \rightarrow N_2(^1\Sigma_g^+) + NH(^1\Delta) \quad (1)$$

$$\rightarrow N_3(^2A', ^2A'') + H \quad (2)$$

$$\rightarrow HN_2(^2A') + N(^2D) \quad (3)$$

as well as the spin-forbidden dissociation to NH($^3\Sigma^-$) have been studied experimentally[2−7] using different techniques, with the exception of the channel in eq 3 due to the high energy required to break the terminal NN bond and form the metastable HN_2 radical.

Theoretically, the spin-allowed and spin-forbidden dissociations in the lowest electronic states into N_2 + NH have been investigated by different authors.[8−10] Specifically, Alexander et al.[10] provided an accurate prediction of the relevant geometries and energies of the barriers for dissociation, using the multireference configuration interaction method with Davidson's correction, MRCI(Q).[11,12]

Dissociation of the excited states has also been studied, with photodissociation experiments conducted[13−17] for the channel in eq 1 showing large differences in the rotational population of the products. The channel in eq 2, which involves higher energies, has also been assessed[18−21] using shorter wavelengths. Theoretically, it was shown[22] that such photodissociation involves mainly the lowest excited singlet state ($1^1A''$), with ab initio calculations being employed to explain the experimentally observed results. More recently, Fang[23] analyzed this process by performing ab initio calculations on the $^1A'$, $^1A''$, and $^3A''$ states. He carried out optimizations of the stationary structures by constraining the system to C_s symmetry from complete active-space self-consistent field calculations (CASSCF) with a reduced active space (8 valence electrons in 7 active orbitals CASSCF(8,7)), the energies being refined using the multireference MP2 approach.[24] Furthermore, two-dimensional quantum mechanical wavepacket calculations of the photodissociation dynamics were performed by Cook et al.[25] using a potential energy surface (PES) constructed with the state-averaged (both the $\tilde{X}^1A'$ and $\tilde{A}^1A''$ carried an equal weight) CASSCF approach in order to support their experimental findings.[21]

After the first experimental evidence on production of cyclic N_3 isomer (cyc-N_3),[26] a nitrogen ring-closing mechanism from photodissociation of HN_3 was studied by Zhang et al.,[27] showing experimental evidence of the formation of cyc-N_3. A theoretical description of the reaction path has also been reported using the full valence CASSCF(16,13) approach with the correlation-consistent[28,29] basis set cc-pV*T*Z, followed by energy refinement with MRCI(Q)/aug-cc-pV*T*Z calculations.

Despite all theoretical efforts to understand the chemistry of the hydrazoic acid, the barriers for dissociation in the excited singlet state lack accurate theoretical prediction to compare with the experimental values, and the whole topology of the

Received: February 28, 2013
Revised: April 12, 2013
Published: April 15, 2013

ground PES remains as yet unexplored. Furthermore, most previous calculations are constrained to planar geometries and do not report harmonic vibrational frequencies. The aim of this work is to provide a detailed and accurate analysis of the structure and energetics of both ground and excited singlet states, which, for symmetric configurations, belong to the A′ and A″ symmetries, respectively. This will include nonplanar configurations, contributing to the understanding of the possible reaction paths and making a first step toward the construction of a global analytical representation. The paper is organized as follows. Section 2 describes the ab initio calculations and extrapolation schemes, while sections 3−6 gather the major results. The conclusions are in section 7.

2. AB INITIO CALCULATIONS AND EXTRAPOLATION SCHEME

Geometry optimizations at the CASSCF level have been performed in the C_1 symmetry point group by considering all six degrees of freedom of the system with basis sets of the correlation-consistent family.[28,29] Preliminary calculations were performed with the VDZ basis set (the cc-pVXZ and aug-cc-pVXZ basis will be abbreviated hereafter as VXZ and AVXZ, respectively; X is the cardinal number), including the quadratic steepest descent reaction path following, in order to understand the connections between the predicted transition states and local minima. However, the geometries reported in this work as well as harmonic vibrational frequencies were obtained at the CASSCF/AVQZ level, where only the 1s orbitals of the nitrogen atoms were kept doubly occupied and, hence, the active space consisted of 16 electrons in 13 molecular orbitals (16,13). Because the optimization is performed in C_1 symmetry, the excited structures had to be optimized as the upper state in a two-state averaged CASSCF calculation, while the ground state was optimized via single-state calculations. On each stationary structure found, the energy was refined by single-point calculations (in C_s symmetry) via the MRCI(Q)[11,12] method, with AVTZ and AVQZ basis sets, followed by extrapolation to the complete basis set (CBS) limit. This is a soundful approach that has recently been shown[30−33] to give excellent results for the HO_x radicals and advocated to be of general utility.

The extrapolation of the raw CASSCF energies has been performed with the two-point protocol proposed by Karton and Martin[34] (originally utilized for the Hartree−Fock energies but shown[35] to perform accurately also for the CASSCF energy)

$$E_X^{\mathrm{CAS}}(\mathbf{R}) = E_\infty^{\mathrm{CAS}}(\mathbf{R}) + B/X^{5.34} \tag{4}$$

where the basis sets are indicated by subscripts (the CBS limit corresponds to $X = \infty$) and $\mathbf{R}$ is a six-dimensional vector describing the geometry. Such extrapolations are carried out pointwisely, with E_∞^{CAS} and B being parameters to be determined from a fit to the AVTZ and AVQZ energies.

To extrapolate the dynamical correlation for systems with a large number of electrons, where calculations with a basis set larger than quadruple-ζ are unaffordable, the uniform singlet- and triplet-pair extrapolation[35] (USTE) method has been used because this has been shown to consistently perform better than traditional schemes (see, e.g., the original paper). In the present approach, the extrapolated dynamical correlation energy (E_∞^{dc}) is obtained from a fit to the pair (T,Q) of raw ones (thus obtained with the AVTZ and AVQZ basis) by using the form

$$E_X^{\mathrm{dc}} = E_\infty^{\mathrm{dc}} + \frac{A_3}{(X-3/8)^3} + \frac{A_5^{(0)} + cA_3^n}{(X-3/8)^5} \tag{5}$$

which provides E_∞^{dc} and A_3; the parameters $A_5^{(0)}$, c, and n have been shown elsewhere[35] to be independent of the system and determined universally for a given post-Hartree−Fock method. These are listed in Table 1 for the coupled cluster and MRCI methods.

Table 1. USTE Extrapolation Parameters[35]

method	$A_5^{(0)}[E_h]$	$c[E_h^{1-(n)}]$	n
MRCI	0.0037685459	−1.17847713	1.25
CCSD	0.16606993	−1.42225121	1.00

In regions close to the minima, where the system may be described by single-reference-based methods, coupled cluster singles and doubles with perturbative triples (CCSD(T)[36]) as well as density functional theory (DFT) calculations were performed. All calculations have been carried out using the MOLPRO package.[37]

3. DECOMPOSITION OF HN_3

The structure of the HN_3 molecule at equilibrium (hereafter set as the reference energy) has been optimized through CASSCF/AVQZ and CCSD(T)/AVTZ calculations. Table 2 shows that

Table 2. Geometry and Vibrational Frequencies of HN_3 at Equilibrium

	exp.[38,39]	CAS/AVQZ	CCSD/AVTZ	ref 23[a]
$R_{N_1N_2}/a_0$	2.143	2.144	2.147	2.149
$R_{N_2N_3}/a_0$	2.349	2.374	2.361	2.349
R_{HN_3}/a_0	1.918	1.940	1.926	1.910
$H\hat{N}_3N_2$/deg	108.8	107.5	108.5	107.3
$N_1\hat{N}_2N_3$/deg	171.3	171.5	171.3	173.7
$\omega_1/\mathrm{cm}^{-1}$	527	524	522	
$\omega_2/\mathrm{cm}^{-1}$	587	600	590	
$\omega_3/\mathrm{cm}^{-1}$	1151	1153	1169	
$\omega_4/\mathrm{cm}^{-1}$	1265	1313	1286	
$\omega_5/\mathrm{cm}^{-1}$	2140	2184	2193	
$\omega_6/\mathrm{cm}^{-1}$	3497	3394	3494	
ZPE/kcal mol^{-1}	13.10	13.10	13.23	

[a]At the CASSCF(8,7)/VDZ level of theory.

both methods agree nicely with the experimental values.[38,39] As expected, the equilibrium structure is well-described by the single-reference coupled cluster method, with the inclusion of dynamical correlation providing a minor improvement over the CASSCF geometries. We have also performed a single-point MRCI(Q)/AVTZ calculation at both the experimental geometry and the point optimized by CASSCF/AVQZ, with the difference found to be only of 0.002 kcal mol^{-1}, which, as noted above, supports the procedure[30−33] utilized in the present work for optimizing the geometries.

In order to assess the accuracy of the ab initio results, we compare our prediction of the H−N_3 bond energy with the accurate experimental measurement[21] using the technique of H-atom Rydberg photofragment translational spectroscopy. As can be seen from Table 3, our CBS extrapolated result of 87.94

dx.doi.org/10.1021/jp402090s | J. Phys. Chem. A 2013, 117, 4044−4050

Table 3. Dissociation Energies (in kcal mol^{-1}) Relative to the Global Minimum, Including Other Results[10,21,23,27,40,41a]

	ZPE	CAS/AVQZ	MRCI(Q)/AVTZ	MRCI(Q)/AVQZ	CBS/MRCI(Q)	exp.	other
H + N_3(lin)	5.83[b]	79.69(72.42)	93.78(83.51)	94.63(87.63)	95.21(87.94)	88.54 ± 0.14[d]	87.7,[e] 85.3[f]
H + cyc-N_3	3.91[b]	116.10(106.91)	126.04(116.85)	127.64(118.45)	128.67(119.48)		117[f]
N + HN_2	8.37[c]	152.41(147.68)	157.00(152.27)	159.50(154.77)	161.11(156.38)		

[a]The results in parentheses are ZPE-corrected. [b]Reference 40. [c]Reference 41. [d]Reference 21. [e]Reference 10. [f]Reference 23. [f]Reference 27.

Table 4. Properties of the Stationary Points for the Ground-State PES[a]

	S_2	$M_{C_{2v}}$	S_3	M_{C_s}	S_4
$R_{N_1N_2}/a_0$	2.390	2.419	2.583	2.958	3.885
$R_{N_2N_3}/a_0$	2.390	2.419	2.583	2.958	3.885
R_{HN_2}/a_0	2.000	1.952	1.938	1.956	1.966
$N_1\hat{N}_2N_3$/deg	159.6	101.9	76.87	45.20	31.67
$H\hat{N}_2N_3$/deg	100.2	129.1	120.4	101.1	90.21
$H\hat{N}_2N_1$/deg	100.2	129.1	120.4	101.1	90.21
ω_1/cm^{-1}	350	486	690	569	322
ω_2/cm^{-1}	468i	861	953	716	391i
ω_3/cm^{-1}	630	1165	1135	1030	400
ω_4/cm^{-1}	1024	1392	1225	1433	1031
ω_5/cm^{-1}	1585	1530	1539i	1715	2131
ω_6/cm^{-1}	3141	3274	3394	3259	3254
ZPE	9.62	12.45	10.58	12.47	10.20
CAS/AVQZ	96.23	86.98	110.93	39.70	52.92
MRCI(Q)/AVTZ	90.06	83.31	101.74	38.31	57.01
MRCI(Q)/AVQZ	91.28	84.32	103.55	39.34	58.56
CBS/MRCI(Q)	92.04	84.99	104.66	39.95	59.54
CBS/MRCI(Q) + ZPE	88.56	84.34	102.14	39.32	56.64
Cho et al.[42]	86.9	78.1	118.6	37.7	

[a]Geometry and vibrational frequencies at the CASSCF/AVQZ level and energies are given in kcal mol^{-1} relative to the global minima.

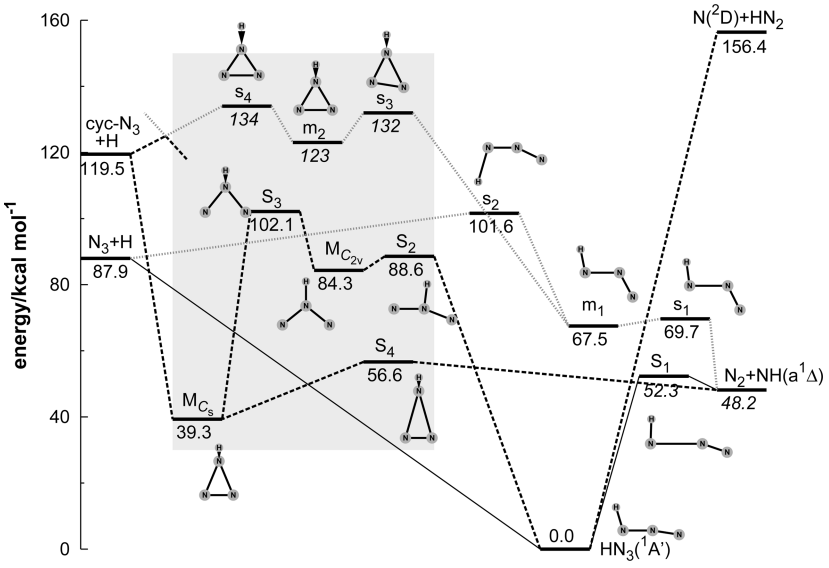

Figure 1. Potential energy profile at the CBS/MRCI(Q) level of theory, including ZPE corrections. The solid lines connecting the structures correspond to the main dissociation paths in the ground state, while the dashed ones are theoretically proposed. The gray dotted lines are relative to the upper state, and the numbers in italic are not at the CBS level.[10,27].

kcal mol^{-1} differs from the experimental value by only 0.6 kcal mol^{-1}, while the error in the measurement is ±0.14 kcal mol^{-1}. Such accuracy can therefore be expected for the other energies calculated in this work, where no experimental data are available. It is worth noting that the results of Alexander et al.,[10] performed before this experimental measurement, compare similarly well, with a deviation of 0.8 kcal mol^{-1}; thus, the N_2 + NH dissociation energy as well as the barrier for this channel calculated in that work can be expected to be of similar accuracy. Because this channel has already been analyzed[8−10] thoroughly by ab initio methods, we do not make any further calculations there.

For the dissociation energy relative to the cyc-N_3 asymptote, our CBS extrapolation of 119.5 kcal mol^{-1} differs from the

dx.doi.org/10.1021/jp402090s | J. Phys. Chem. A 2013, 117, 4044−4050

value of Zhang et al.[27] by 2.5 kcal mol^{-1} at the MRCI(Q)/AVTZ level, a result that we have also reproduced in Table 3 in order to extrapolate to the CBS limit. To the best of our knowledge, there is no prediction of the HN_2 + N dissociation energy available in the literature; it is calculated here at the CBS/MRCI(Q) limit. The enormous energy required to open this channel makes the HN_2 radical very unstable in reaction with atomic hydrogen. Indeed, our CASSCF calculations suggest that this reaction occurs without a barrier if the NÑN bond angle is strongly bent from its nearly linear structure at the equilibrium HN_3 molecule. In fact, for ground-state HN_3, the only barrier in the exit channels seems to be the one relative to N_2 + NH dissociation.[10]

4. STATIONARY STRUCTURES AND REACTION PATHS IN THE GROUND STATE

The stationary structures found in this work and their properties are gathered in Table 4, while an overview of the stationary structures and reaction paths on both ground and excited potential energy surfaces of HN_3 is displayed in the energy diagram of Figure 1, which shows the predicted structures from this work together with others previously reported.[10,23,27] M stands for minimum and S for saddle point, while the upper-state counterparts have the same notation as those in the lower case.

As can be seen, starting from the equilibrium structure of HN_3 in its nearly linear trinitrogen shape and following the reaction path for bending the NÑN angle, a saddle point (S_2) is reached corresponding to a hydrogen atom migration from a terminal nitrogen to the central one with an energy of 88.56 kcal mol^{-1} above the global minimum (unless mentioned otherwise, the energies given in this discussion are CBS/MRCI(Q) including the zero-point energy (ZPE) correction relative to the global minimum). This saddle point is a first-order transition state, with an imaginary frequency of 468 cm^{-1} that corresponds to a planar HÑN bending mode. Following the minimum-energy path, a local metastable C_{2v} minimum ($M_{C_{2v}}$) is obtained lying at 84.34 kcal mol^{-1} and with a metastability of 4.22 kcal mol^{-1}. It is interesting to note that for these two structures, and subsequent ones, the NH bond length is similar to its value on the separated imidogen molecule, with the fundamental vibration corresponding to the stretching mode of this bond (ω_6) lying also close to the fundamental in isolated imidogen (~3200 cm^{-1}).

With further bending of the NÑN angle from the $M_{C_{2v}}$ structure, a nonplanar saddle point is reached (S_3). It belongs to the C_s point group due to a plane of symmetry cutting the NH bond and lies 17.8 kcal mol^{-1} above $M_{C_{2v}}$. From Table 4, one can clearly see that while the NÑN angle progressively decreases, both NN bond lengths slowly increase when following this reaction path. It is thus fair to expect that it will lead to dissociation to cyc-N_3, which has a bond angle of 49.2° and two bond distances of 2.8 a_0. The imaginary frequency of the S_3 transition state corresponds to a simultaneous bend of both NÑN and HÑN angles without loosing the C_s plane of symmetry.

The final step toward dissociation to cyc-N_3, passes through a relatively deep minimum that has also a nonplanar C_s structure (M_{C_s}). Interestingly, the NÑN angle and NN bond lengths in M_{C_s} exceed the values of the final cyc-N_3 form, and thus, the progressive change in these variables (observed through this path) cannot be observed in this way. In fact, the NH bond length in M_{C_s} shows that it is a highly bound feature rather than a mere structure along the dissociation path. Thus, M_{C_s} may be thought of as a stable structure formed from the abstraction of a H atom by cyc-N_3. The CASSCF calculations show that this abstraction reaction occurs without an energy barrier, suggesting that cyc-N_3 can easily recombine with H atoms to generate the M_{C_s} isomer.

The reactivity of cyc-N_3 with some atmospheric species has been considered theoretically[43,44] in order to assess its stability. Although the cyc-N_3 + H_2O reaction has shown large barriers,[44] it was found to lead to cyc-N_3H + OH, which seems to correspond to the M_{C_s} here reported. However, a previously unknown nonplanar transition state (S_4) (which connects M_{C_s} directly with the N_2 + NH($^1\Delta$) fragments) was found in this work and indicates that such an isomer may dissociate, especially if formed with a large energy content as would be the case in the cyc-N_3 + H reaction. Although no experiments have been carried out for this process, it seems that this isomer of HN_3 could be detected experimentally from N_2 + NH($^1\Delta$) collisions.

During the course of this work, another group also found the S_2, $M_{C_{2v}}$, S_3, and M_{C_s} structures using multireference MP2 calculations.[42] Our results, however, are different in that we give vibrational frequencies and ZPE corrections (which are fundamental for comparing with the experiments) and are also more reliable due to their CBS/MRCI(Q) nature.

Further geometry optimizations have been performed at the CCSD(T)/AVTZ level followed by extrapolating the energy using the USTE(T,Q) method in order to compare with previous results. Due to its single-reference nature, the CCSD(T) optimizations often find convergence problems, and only the two new minima are examined at this level, with the results presented in Table 5. The validity of the CCSD(T) approach is analyzed with the T1 and D1 diagnostics[45−47] and also by inspecting the coefficient of the dominant configuration in the CI vector of a CASSCF/AVQZ calculation. It is clear from Table 5 that the M_{C_s} structure is more suitably described

Table 5. Optimized Minima at the CCSD(T) and DFT Levels (without ZPE correction) Using the AVTZ basis. Energies in kcal mol^{-1} Relative to the Global Minima

	CCSD(T)		DFT	
	$M_{C_{2v}}$	M_{C_s}	$M_{C_{2v}}$	M_{C_s}
$R_{N_1N_2}/a_0$	2.412	2.926	2.373	2.922
$R_{N_2N_3}/a_0$	2.413	2.926	2.373	2.922
R_{HN_2}/a_0	1.937	1.941	1.954	1.938
$N_1\hat{N}_2N_3$/deg	100.4	45.77	96.32	45.04
$H\hat{N}_2N_3$/deg	129.8	101.7	131.8	102.3
$H\hat{N}_2N_1$/deg	129.8	101.7	131.8	102.3
T1	0.026	0.015		
D1	0.075	0.033		
CI coeff.[a]	0.882	0.931		
AVTZ	85.67	37.99	97.29	46.11
AVQZ	86.61	38.91		
CBS	87.23	39.45		

[a]Coefficient of the dominant configuration on the CI vector as calculated at the CASSCF/AVQZ level.

dx.doi.org/10.1021/jp402090s | J. Phys. Chem. A 2013, 117, 4044−4050

by a single configuration than $M_{C_{2v}}$ due to its lower T1 and D1 values and larger coefficient of the dominant configuration (note that $M_{C_{2v}}$ was even found to slightly deviate from its symmetric configuration). Although a general good agreement between the MRCI(Q) and CCSD(T) energies is obtained, the $M_{C_{2v}}$ values show larger differences than M_{C_s}, which is not surprising due to the above-mentioned multireference character.

Although the MRCI(Q) energies obtained in this work provide accurate ab initio estimates, it is currently unaffordable to calculate a grid over the whole configurational space to obtain a global analytical representation. Therefore, the values here reported offer benchmark results to asses the validity of different DFT functionals or other cost-effective approaches for a future calculation and modeling of the whole potential energy surface. Preliminary calculations employing the B3LYP[48] functional (which has been considered appropriate to calculate the geometry and fundamental frequencies of HN_3 at equilibrium[49]) were performed on the $M_{C_{2v}}$ and M_{C_s} structures, also using the AVTZ basis set for consistency. The results show reasonable agreement with the CASSCF geometries and vibrational frequencies, but the calculated energy differs appreciably, as shown in Table 5.

5. EXCITED SINGLET STATE

After the system is photoexcited to the $\tilde{A}^1A''$ state, decomposition follows quickly given the energy content of the excited molecule. The lowest-energy decomposition (see eq 1) leads to N_2 + NH($^1\Delta$), and the experiments[14,16,17] suggest that it occurs directly without a strong potential barrier along the HN−NN bond distance. This has been corroborated by early theoretical calculations,[22] although Fang[23] has found a small barrier of 0.2 kcal mol^{-1} (including ZPE correction) at the CASPT2 level, arguing that it was not inconsistent with the experiments. Note that the absence of such a barrier leads to the conclusion that there is no true minimum in this region of the excited-state PES. Note further that prior to the above-mentioned work, there was no information (theoretical or experimental) about this structure. More recent and accurate calculations with a larger active space have reported such a minimum,[27] thus corroborating the existence of the barrier. Indeed, our CASSCF(16,13)/AVQZ results also predict this transition state (named s_1) with an imaginary frequency of 589 cm^{-1}, while the CBS/MRCI(Q) calculations show it to lie 2.2 kcal mol^{-1} above the trans minimum (Table 6).

The dissociation to N_3 + H is believed to occur through a reaction barrier in the excited state (s_2) rather than through internal conversion to the $^1A''$ or $^3A''$ states, which was experimentally measured to be 13.15 ± 2.29 kcal mol^{-1} above the dissociation channel.[21] Previous theoretical work on this barrier shows some disagreement, with Lock et al.[20] predicting it to be >3.3 kcal mol^{-1}, while Fang's[23] calculations yield 27.9 kcal mol^{-1}. Our best result at the CBS/MRCI(Q) level of 13.70 kcal mol^{-1} shows perfect agreement with the experimental value, thus validating the employed methodology (see also elsewhere[30−33]) also for the upper state.

Between the above two barriers lies therefore the $HN_3(^1A'')$ minimum, which has a trans configuration with the NNN moiety further from linearity than that for the ground state. This implies that if the system is excited from the region of the ground-state minimum to the correspondent Franck−Condon region of the upper PES, it will experience a considerable gradient in this coordinate.[22] This minimum has also a cis counterpart that, to the best of our knowledge, has not been optimized before. Our results show it to lie only 1.7 kcal mol^{-1} above the trans and showing bond lengths similar to it. Interestingly, an isomerization transition state on the torsion coordinate does not seem to exist, although a one-dimensional cut along this coordinate shows a maximum with ∠HNNN = 90°. This happens because such a maximum is not a real transition state if the NN coordinate (leading to dissociation) is considered. The cis and trans isomer dissociation paths are thus independent, with the dissociation for ∠HNNN fixed at 90° showing a decay in energy with no stationary structure.

The region of the excited PES corresponding to structures with the NNN angle largely in cyclic form was studied by Zhang et al.[27] and is displayed in Figure 1. In their study, a mechanism for explaining the formation of cyc-N_3 in photodissociation was proposed through ab initio calculations. This process involves however a first excitation from the ground to a third excited singlet state followed by internal conversion to the excited state studied in this work, through a conical intersection and subsequent bond cleavage, as shown in Figure 1.

Table 6. Properties of the Excited-State Stationary Points[a]

	m_1-trans	m_1-cis	s_1	s_2
$R_{N_1N_2}/a_0$	2.248	2.254	2.194	2.248
$R_{N_2N_3}/a_0$	2.749	2.763	3.073	2.352
R_{HN_3}/a_0	1.959	1.974	1.963	2.768
$N_1\hat{N}_2N_3$/deg	120.2	119.3	118.9	155.9
$H\hat{N}_3N_2$/deg	101.2	102.9	97.38	106.6
∠HNNN/deg	180.0	0.0	180.0	0.0
ω_1/cm^{-1}	433	245	257	471
ω_2/cm^{-1}	508	468	475	526
ω_3/cm^{-1}	648	642	589i	898
ω_4/cm^{-1}	1337	1347	1188	1162
ω_5/cm^{-1}	1700	1670	1751	1614
ω_6/cm^{-1}	3272	3166	3256	1770i
ZPE	11.29	10.78	9.90	6.68
CAS/AVQZ	72.63	74.08	74.16	105.9
MRCI(Q)/AVTZ	67.32	69.51	70.44	106.2
MRCI(Q)/AVQZ	68.53	70.74	71.93	107.3
CBS/MRCI(Q)	69.31	71.52	72.87	108.1
CBS/MRCI(Q)+ZPE	67.50	69.20	69.67	101.6
exp.[21]				101.7 ± 2.4

[a]Geometry and vibrational frequencies at the CASSCF/AVQZ level and energies given in kcal mol^{-1} relative to the global minima.

6. SURFACE CROSSINGS

The presence of surface crossings could change the picture of the direct photodissociation in the upper state. For example, in case there is a crossing between ground and excited singlet states, the excited molecule could cross back to the ground state and dissociate from there. This mechanism was considered by Fang[23] for the dissociation to N_2 + NH($^1\Delta$), where one such intersection was found and optimized in state-averaged CASSCF(8,7)/VDZ calculations, but the conclusion was that this is not a probable event given that the crossing lies higher in energy than s_1. We have also searched for crossings between the two PESs in several regions of configurational space but rarely found them. Indeed, even the crossing reported by Fang[23]

dx.doi.org/10.1021/jp402090s | J. Phys. Chem. A 2013, 117, 4044−4050

could not be supported, except if reducing the active space to CASSCF(10,10); see Figure 2. We therefore believe that the reduced active space CASSCF(8,7) utilized by Fang[23] is not suitable for this part of the PES.

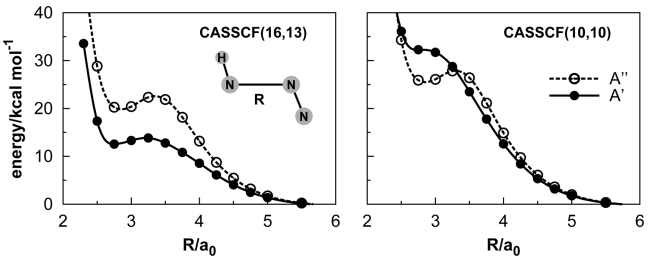

Figure 2. CASSCF/VDZ energy profile along the NN bond length showing the incorrect behavior of the calculations with reduced active space.

The only region of the PES where we have found crossings is close to dissociation to the N_3 fragment. The linear form of N_3 is Renner−Teller degenerate (see eqs 1 and 3), and the interaction with the H atom splits the degeneracy into the two singlet sheets here considered (ignoring the triplet states). On the other hand, the cyc-N_3 fragment is nondegenerate and correlates only to ground singlet state (which for some configurations may not correspond to the A′ symmetry due to the presence of crossings), and therefore, a dissociation path from the excited state to cyc-N_3 must find a surface intersection, as indicated in Figure 1. Due to the complexity of the electronic states of the N_3 fragment for different bond angles,[40,50] we have found several crossings close to the dissociation into this channel, which occurs for highly symmetric attacks of the H atom ($C_{\infty v}$, C_{2v}, and C_{3v}). For example, Figure 3 shows the C_{2v} approach of a H atom with the

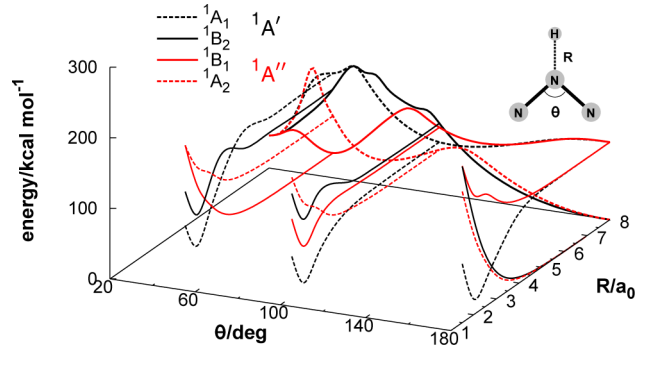

Figure 3. CASSCF/VDZ cuts for the dissociation to N_3 + H restricting to C_{2v} geometries and optimizing the NN bond lengths for each point. The back part of the graph shows the optimized bending curve for the dissociated N_3.

NN bond lengths being relaxed; A′ states are in black, and A″ states are in red. Note though that the minimum-energy path for the cyc-N_3 + H reaction proceeds without a barrier through a non-C_{2v} path (A′ symmetry). For other symmetrical parts of the PES, such as the ground state near S_2 and S_3, we have found no crossings between the two PESs. Although there are crossings between higher excited states, the two PESs here considered appear to be well-separated at the strong interaction region, which is quite unusual for polyatomics.

7. CONCLUDING REMARKS

We have investigated the stationary structures and reaction paths of ground- and excited-singlet PESs of the hydrazoic acid using state-of-the-art ab initio calculations with CBS extrapolation. Comparison with two recent experimental measurements shows chemical accuracy, which validates the employed methodologies. Indeed, the accuracy of our predictions should hold for other structures with no experimental counterpart. Among the results, we have predicted minima and transition states in the ground-state PES, as well as a description for the H-abstraction reaction of cyc-N_3. With geometries and vibrational frequencies optimized at the full-valence CASSCF/AVQZ level and energies refined with MRCI(Q) followed by CBS extrapolation,[30−33] the results here reported offer a benchmark to test the validity of other approaches in describing the global representation of the PES, namely, single-reference-type ones such as DFT and coupled cluster.

AUTHOR INFORMATION

Corresponding Author

*E-mail: varandas@qtvs1.qui.uc.pt.

Notes

The authors declare no competing financial interest.

ACKNOWLEDGMENTS

This work is financed by FEDER through "Programa Operacional Factores de Competitividade - COMPETE" and national funds under the auspices of Fundação para a Ciência e a Tecnologia, Portugal (Projects PTDC/QUI-QUI/099744/2008, PTDC/AAC-AMB/099737/2008, and SFRH/BD/61229/2009).

REFERENCES

(1) Orlando, J. J.; Tyndall, G. S.; Betterton, E. A.; Lowry, J.; Stegall, S. T. Atmospheric Chemistry of Hydrazoic Acid (HN_3): UV Absorption Spectrum, HO• Reaction Rate, and Reactions of the •N_3 Radical. *Environ. Sci. Technol.* **2005**, *39*, 1632−1640.

(2) Kajimoto, O.; Yamamoto, T.; Fueno, T. Kinetic Studies of the Thermal Decomposition of Hydrazoic Acid in Shock Waves. *J. Chem. Phys.* **1979**, *83*, 429−435.

(3) Stephenson, J. C.; Casassa, M. P.; King, D. S. Energetics and Spin- and Λ-Doublet Selectivity in the Infrared Multiphoton Dissociation $DN_3 \rightarrow DN(X^3\Sigma^-,a^1\Delta) + N_2(X^1\Sigma_g^+)$: Experiment. *J. Chem. Phys.* **1988**, *89*, 1378−1387.

(4) Foy, B. R.; Casassa, M. P.; Stephenson, J. C.; King, D. S. Unimolecular Dynamics Following Vibrational Overtone Excitation of HN_3 $v_1 = 5$ and $v_1 = 6$: $HN_3(X;v,J,K) \rightarrow HN(X^3\Sigma^-;v,J,\Omega)+N_2(X^1\Sigma_g^+)$. *J. Chem. Phys.* **1988**, *89*, 608−609.

(5) Foy, B. R.; Casassa, M. P.; Stephenson, J. C.; King, D. S. Dissociation Lifetimes and Level Mixing in Overtone-Excited $HN_3(X^1A')$. *J. Chem. Phys.* **1989**, *90*, 7037−7045.

(6) Chen, J.; Quiñones, E.; Dagdigian, P. J. Observation of $NH(a^1\Delta,v = 1)$ from the H+N_3 Reaction. *J. Chem. Phys.* **1989**, *90*, 7603−7604.

(7) Foy, B. R.; Casassa, M. P.; Stephenson, J. C.; King, D. S. Overtone-Excited HN3(X^1A'): Anharmonic Resonance, Homogeneous Linewidths, and Dissociation Rates. *J. Chem. Phys.* **1990**, *92*, 2782−2789.

(8) Yarkony, D. R. Spin−Orbit Effects in the Decomposition Reaction $N_3H(^1A') \rightarrow N_2(X^1\Sigma_g^+)+NH(X^3\sigma^-,a^1\Delta)$. *J. Chem. Phys.* **1990**, *92*, 320−323.

(9) Alexander, M. H.; Werner, H.-J.; Dagdigian, P. J. Energetics and Spin- and Λ-Doublet Selectivity in the Infrared Multiphoton Dissociation $DN_3 \rightarrow DN(X^3\Sigma^-,a^1\Delta) + N_2(X^1\Sigma_g^+)$: Theory. *J. Chem. Phys.* **1988**, *89*, 1388−1400.

(10) Alexander, M. H.; Werner, H.-J.; Hemmer, T.; Knowles, P. J. Ab initio Study of the Energetics of the Spin-Allowed and Spin-Forbidden Decomposition of HN_3. *J. Chem. Phys.* **1990**, *93*, 3307−3318.
(11) Werner, H.-J.; Knowles, P. J. An Efficient Internally Contracted Multiconfiguration−Reference Configuration Interaction Method. *J. Chem. Phys.* **1988**, *89*, 5803−5814.
(12) Werner, H.-J.; Knowles, P. J. An Efficient Method for the Evaluation of Coupling Coefficients in Configuration Interaction Calculations. *Chem. Phys. Lett.* **1988**, *145*, 514−522.
(13) Rohrer, F.; Stuhl, F. The 193 (and 248) nm Photolysis of HN_3: Formation and Internal Energy Distributions of the NH($a^1\Delta$,$b^1\Sigma^+$, $A^3\Pi$, and $c^1\Pi$) States. *J. Chem. Phys.* **1988**, *88*, 4788−4799.
(14) Chu, J. J.; Marcus, P.; Dagdigian, P. J. Onecolor Photolysis−Ionization Study of HN_3: The N_2 Fragment Internal Energy Distribution and μ-v-J Correlations. *J. Chem. Phys.* **1990**, *93*, 257−267.
(15) Gericke, K.-H.; Theinl, R.; Comes, F. J. Vector Correlations in the Photofragmentation of HN_3. *J. Chem. Phys.* **1990**, *92*, 6548−6555.
(16) Gericke, K.-H.; Haas, T.; Lock, M.; Theinl, R.; Comes, F. J. Hidrazoic Acid ($\tilde{A}^1A''$) Hypersurface at Excltation Energies of 4.0−5.0 eV. *J. Phys. Chem.* **1991**, *95*, 6104−6111.
(17) Hawley, M.; Baronavski, A. P.; Nelson, H. H. Vibrational Distributions of NH($a^1\Delta$) from the Photolysis of HN_3 from 220−290 nm. *J. Chem. Phys.* **1993**, *99*, 2683−2642.
(18) Gericke, K.-H.; Lock, M.; Comes, F. J. Photodissociation of HN_3: Direct Formation of Hydrogen Atoms. *Chem. Phys. Lett.* **1991**, *186*, 427−430.
(19) Haas, T.; Gericke, K.-H.; Maul, C.; Comes, F. J. Photodissociation Dynamics of HN_3. The N_3 Fragment Internal Energy Distribution. *Chem. Phys. Lett.* **1993**, *202*, 108−114.
(20) Lock, M.; Gericke, K.-H.; Comes, F. J. Photodissociation Dynamics of $HN_3+h\nu\rightarrow H+N_3$. *Chem. Phys.* **1996**, *213*, 385−396.
(21) Cook, P. A.; Langford, S. R.; Ashfold, M. N. R. The Ultraviolet Photodissociation of HN_3: The H + N_3 Product Channel. *Phys. Chem. Chem. Phys.* **1999**, *1*, 45−55.
(22) Meiert, U.; Staemmler, V. CASSCF and CEPA Calculations for the Photodissociation of HN_3. 2. Photodissociation Into N_2 and NH on the Lowest $^1A''$ Surface of HN_3. *J. Phys. Chem.* **1991**, *95*, 6111−6117.
(23) Fang, W.-H. Photodissociation of HN_3 at 248 nm and Longer Wavelength: A CASSCF Study. *J. Phys. Chem. A* **2000**, *104*, 4045−4050.
(24) McDouall, J. J. W.; Peasley, K.; Robb, M. A. A Simple MCSCF Perturbation Theory: Orthogonal Valence Bond Møller−Plesset 2 (OVB MP2). *Chem. Phys. Lett.* **1988**, *148*, 183−189.
(25) Cook, P. A.; Jimeno, P.; Ashfold, M. N. R.; Balint-Kurti, G. G.; Dixon, R. N. An Ab Initio Study of the Photodissociation of HN_3 Molecules Following Excitation in the $\tilde{A}^1A'' \leftarrow {}^1A'\tilde{X}$ Absorption System. *Phys. Chem. Chem. Phys.* **2002**, *4*, 1513−1521.
(26) Hansen, N.; Wodtke, A. M. Velocity Map Ion Imaging of Chlorine Azide Photolysis: Evidence for Photolytic Production of Cyclic-N_3. *J. Phys. Chem. A* **2003**, *107*, 10608−10614.
(27) Zhang, J.; Zhang, P.; Chen, Y.; Yuan, K.; Harich, S. A.; Wang, X.; Wang, Z.; Yang, X.; Morokuma, K.; Wodtke, A. M. An Experimental and Theoretical Study of Ring Closing Dynamics in HN_3. *Phys. Chem. Chem. Phys.* **2006**, *8*, 1690−1696.
(28) Dunning, T. H. Gaussian Basis Sets for Use in Correlated Molecular Calculations. I. The Atoms Boron through Neon and Hydrogen. *J. Chem. Phys.* **1989**, *90*, 1007−1023.
(29) Kendall, R. A.; Dunning, T. H., Jr.; Harrison, R. J. Electron Affinities of the First-Row Atoms Revisited. Systematic Basis Sets and Wave Functions. *J. Chem. Phys.* **1992**, *96*, 6796−6806.
(30) Varandas, A. J. C. Is HO_3 Minimum Cis or Trans? An Analytic Full-Fimensional Ab Initio Isomerization Path. *Phys. Chem. Chem. Phys.* **2011**, *13*, 9796−9811.
(31) Varandas, A. J. C. On the Stability of the Elusive HO_3 Radical. *Phys. Chem. Chem. Phys.* **2011**, *13*, 15619−15623.
(32) Varandas, A. J. C. Ab Initio Treatment of Bond-Breaking Reactions: Accurate Course of HO_3 Dissociation and Revisit to Isomerization. *J. Chem. Theory Comput.* **2012**, *8*, 428−441.
(33) Varandas, A. J. C. Accurate Determination of the Reaction Course in $HY_2 \rightleftharpoons$ Y + YH (Y = O,S): A Detailed Analysis of the Covalent- to Hydrogen-Bonding Transition. *J. Phys. Chem. A* **2013**, DOI: 10.1021/jp401384d.
(34) Karton, A.; Martin, J. M. L. Comment on: "Estimating the Hartree−Fock Limit From Finite Basis Set Calculations" [Jensen F. (2005) Theor. Chem. Acc. 113, 267]. *Theor. Chem. Acc.* **2006**, *115*, 330−333.
(35) Varandas, A. J. C. Extrapolating to the One-Electron Basis-Set Limit in Electronic Structure Calculations. *J. Chem. Phys.* **2007**, *126*, 244105.
(36) Watts, J. D.; Gauss, J.; Bartlett, R. J. Coupled-Cluster Methods With Noniterative Triple Excitations for Restricted Open-Shell Hartree−Fock and Other General Single Determinant Reference Functions. Energies and Analytical Gradients. *J. Chem. Phys.* **1993**, *98*, 8718−8733.
(37) *MOLPRO*, version 2010.1, A Package of Ab Initio Programs, Werner, H.-J.; Knowles, P. J.; Lindh, R.; Manby, F. R.; M. Schütz, Celani, P.; Korona, T.; et al. http://www.molpro.net (2010).
(38) Winnewisser, B. P. The Substitution Structure of Hydrazoic Acid. *J. Mol. Spectrosc.* **1980**, *82*, 220−223.
(39) Moore, C. B.; Rosengren, K. Infrared Spectrum and Vibrational Potential Function of Hydrazoic Acid. *J. Chem. Phys.* **1966**, *44*, 4108−4115.
(40) Zhang, P.; Morokuma, K.; Wodtke, A. M. High-Level Ab Initio Studies of Unimolecular Dissociation of the Ground-State N_3 Radical. *J. Chem. Phys.* **2005**, *122*, 014106.
(41) Poveda, L. A.; Varandas, A. J. C. Accurate Single-Valued DMBE PES for HN_2. *J. Phys. Chem. A* **2003**, *107*, 7923−7930.
(42) Cho, J.; Lee, H. S.; Choi, C. H. Structural Isomers and Excited States of HN_3. *Bull. Korean Chem. Soc.* **2011**, *32*, 3641−3643.
(43) Yu, X.-F.; Jin, L.; Ding, Y.-H. Theoretical Study on Reactions of Cyclic-N_3 with NO, NO_2 and Cl_2. *J. Mol. Struct.: THEOCHEM* **2009**, *911*, 13−18.
(44) Jin, L.; Yu, X.-F.; Pang, J.-L.; Zhang, S.-W.; Ding, Y.-H. Theoretical Study on the Reactions of the Cyclic Trinitrogen Radical toward Oxygen and Water. *J. Phys. Chem. A* **2009**, *113*, 8500−8505.
(45) Lee, T. J.; Taylor, P. R. A Diagnostic for Determining the Quality of Single-Reference Electron Correlation Methods. *Int. J. Quantum Chem., Symp.* **1989**, *23*, 199−207.
(46) Leininger, M. L.; Nielsen, I. M. B.; Crawford, T. D.; Janssen, C. L. A New Diagnostic for Open-Shell Coupled-Cluster Theory. *Chem. Phys. Lett.* **2000**, *328*, 431−436.
(47) Lee, T. J. Comparison of the T1 and D1 Diagnostics for Electronic Structure Theory: A New Definition for the Open-Shell D1 Diagnostic. *Chem. Phys. Lett.* **2003**, *372*, 362−367.
(48) Stephens, P. J.; Devlin, F. J.; Chabalowski, C. F.; Frisch, M. J. Ab Initio Calculation of Vibrational Absorption and Circular Dichroism Spectra Using Density Functional Force Fields. *J. Phys. Chem.* **1994**, *98*, 11623−11627.
(49) Rosenstock, M.; Rosmus, P.; Reinsch, E. A.; Treutler, O.; Carter, S.; Handy, N. C. Potential Energy Function and Vibrational States of HN_3 and DN_3. *Mol. Phys.* **1998**, *93*, 853−865.
(50) Galvão, B. R. L.; Caridade, P. J. S. B.; Varandas, A. J. C. N($^4S/^2D$)+N_2: Accurate Ab Initio-Based DMBE Potential Energy Surfaces and Surface-Hopping Dynamics. *J. Chem. Phys.* **2012**, *137*, 22A515.